Chin. J. Astron. Astrophys. Vol. 1, No. 6, (2001) 537–548
(http://www.chjaa.org or http://chjaa.bao.ac.cn)

Chinese Journal of
Astronomy and
Astrophysics

A Correlation between Proton Events and Hα Flares and its Possible Interpretation

Kim Jik Su[1,2], Yuan-Yong Deng[1] ⋆, Kim Kum Sok[1,2] and Kim Jin Song[1,2]

[1] National Astronomical Observatories, Chinese Academy of Sciences, Beijing 100012
[2] Pyongyang Astronomical Observatory, Academy of Sciences, DPR of Korea

Received 2001 May 17; accepted 2001 September 14

Abstract Comparing space proton event data obtained during 1970–1980 with their identified Hα flare signatures we discover a peculiar correlation between them, according to which weak and small Hα flares can also produce proton events, and we reveal a characteristic "triangle" distribution of Hα flares accompanying proton events. In order to explain such feature of proton events, we accept the acceleration mechanism by DC electric field. To deduce the parallel electric field we use the electric current helicity (or force-free parameter α) determined by the Huairou vector magnetograph. A comparison of $E_\parallel$ with $E_\perp$ shows that the former is negligible in flaring sites. We show that in the flaring current sheet ion-anisotropy is generated, and it, in turn, gives rise to ion-anisotropic instability which competes with electric acceleration to give one possibility: the acceleration by DC electric field or annihilation of the built-up energy. The competition of DC acceleration and ion-anisotropic instability annihilation in the current sheet gives a possible explanation for the above-mentioned "triangle" character of the distribution.

Key words: Sun: flares — Sun: particle emission

1 INTRODUCTION

It is well known that solar proton flares are mainly correlated with strong, bright H_α flares, in particular, with two ribbon flares. Ellison et al. (1961) were the first to draw attention to the fact that all cosmic-ray flares had the typical two-ribbon shape. Then, Švestka and Simon (1976) drew up the "Catalog of Solar Particle Events, 1956–1969", and using this Catalog, Dodson and Hedeman could safely identify the flare sources for 50 proton events. Out of the 50 identified sources, 45 appeared to be two-ribbon flares (Švestka 1981). From this observation, Švestka concluded "Thus one can reasonably suppose that whereas both the compact flares and two-ribbon flares are seats of the primary acceleration to ~ 100 keV, only in two-ribbon flares can particles be accelerated to much higher energies."

⋆ E-mail: dyy@sun10.bao.ac.cn

Observations aboard spacecraft since the end of the 1960s, however, have shown that even flares as faint and small as SF (Hα flare) may be able to give modest proton events (Molchanov 1984; see below Sect. 2). On the other hand, proton events are believed to be closely connected with Type II bursts (Švestka & Fritzova 1974) and Type II bursts, in turn, are considered to be generated by coronal and interplanetary shocks (Goldman & Smith 1986). This apparent chain of events has convinced researchers that the generation of energetic proton streams is due to coronal shock wave acceleration. According to de Jager (1990), direct electric field generated in initial magnetic reconnection in a current sheet accelerates mainly electrons to $\sim 10\,\mathrm{MeV}$ within 0.1 s; a few seconds later protons trapped by the shock are accelerated to $\sim 100\,\mathrm{MeV}$; finally, the protons can be further accelerated to GeV energies by shock waves in open magnetic fields.

That the principal acceleration of protons is by coronal and interplanetary shocks could also be justified by the fact that as distinct from electrons, the observed energy spectrum of protons fits well to a modified Bessel function-type distribution which may be deduced from stochastic acceleration mechanisms operating in shock waves (McGuire et al. 1981; Ramaty 1979; Barbosa 1979).

Recent observational results, especially, γ-ray line observations and their comparison with hard X-ray and microwave bursts, however, have shown that the proton acceleration at least up to tens of MeV, occurs synchronously with electron acceleration already at the impulsive phase of flare with a time scale less than one second (Forrest & Chupp 1983; Akimov et al. 1991, 1994; Kocharov et al. 1999).

Zhang et al. (1990), Liu & Li (1990), and Li & Wang (1994), based on several observations, confirmed that almost all the proton active regions have magnetic shear configurations. Zhou and Zheng (1998) showed that a common characteristic of active regions that are strong proton flare productive is enhanced rotation of the region.

According to Akimov et al. (1994) and Litvinenko & Somov (1995), acceleration of protons during the late phase of large γ-ray/proton flares to GeV energies can occur in a reconnecting current sheet, formed behind a rising coronal mass ejection or an erupting prominence. The direct electric field, generated in such structures by a rapidly changing magnetic field, is the fastest and easiest means of particle acceleration to relativistic energies (see also Martens 1988).

The existence and importance of shock acceleration in strong flares are undoubted. Note, however, that there are flares in which shock acceleration seems to be unsuitable for interpreting the delayed component of γ-ray emission from neutral pion π^0 decay produced by the protons interacting with the medium, because a shock is too high in the solar corona by the time the delayed component appears. If the protons which later produced the pions are accelerated by the shock, they could not reach the chromosphere and produced the γ-emission.

We assume that the proton acceleration occurs in reconnecting current sheets and is formed in various loci of sheared magnetic configurations, by DC electric field (Martens 1988; Litvinenko & Somov 1995; Litvinenko 1996; Sakai 1992).

Acceleration by DC electric field can be divided into two classes: accelerations along ($E_\parallel$) and across ($E_\perp$) magnetic field. A number of authors pointed out the importance of parallel acceleration by $E_\parallel$ (Schindler, Hesse & Birn 1991; Alfven 1981; Pacini 1975; Priest & Forbes 2000) in the generation of cosmic rays. A non-trivial estimate of the parallel electric field ($E_\parallel$), however, was not always possible (Priest & Forbes 2000).

Recent observations of vector magnetic field make it possible to estimate $E_\parallel$ (see Sect.3 below). Comparing $E_\parallel$ with $E_\perp$ in active regions, we come to the conclusion that the parallel

electric field in the reconnecting site is negligible compared to the perpendicular field.

We argue that besides electric field, an important factor which influences proton acceleration is ion-anisotropy generated by the electric field acceleration, which gives rise to ion-anisotropic instability in a flaring current sheet (Kim 1993).

Using the above-mentioned DC electric field acceleration and ion-anisotropic instability we find a suitable explanation for a correlation between space proton event observations (1970–1980) and related Hα flares.

In Sect. 2, we present the space proton event observation data and reveal a peculiar correlation between the proton events and related Hα flares. In Sect. 3, DC acceleration and the formation of ion-anisotropy are considered. In Sect. 4 ion-anisotropic instability in current sheet is estimated, and a possible interpretation of the observed correlation is given. In Appendix, we give the derivation of a simple relation between the current helicity and the electric field along magnetic field.

2 A CORRELATION BETWEEN SOLAR PROTON EVENTS AND Hα FLARES

In order to ascertain a relation between solar proton events and the Hα signatures of related Hα flares, we have made use of "Solar-Geophysical Data" supplemented by data of the satellite "Meteor" (Molchanov 1984). The Catalog includes data of solar proton events, covering the period from January 1970 (1970–01) to December 1980 (1980–12). The energy range of detection of proton events is 10–100 MeV from 1970–01 to 1973–05, 5–100 MeV from 1973–06 to 1975–06, and 13.7–80 MeV from 1975–08 to 1975–12, and the threshold of detection is 0.1 particle $cm^{-2}s^{-1}sr^{-1}$. We chose only those proton events with a more than 0.7 probability of being identifiable with Hα flares.

Using the above data one can draw up the number distribution of proton events identified with Hα flares given in Table 1.

Table 1 Number Distribution of Proton Events Identified with Hα Flares (1970–1980)

Hα Flare	S	1	2	3
B	**33**	**84**	**57**	**14**
N	**34**	**56**	**21**	2
F	**17**	3	2	0

The number distribution of all the Hα flares in the same period as in Table 1 is given in Table 2 (Vitinsky 1970–1981) (the fractions in parentheses is the ratio of the number of Hα flares accompanying proton events to the total number of Hα flares).

Table 1 shows that Hα flares which accompany proton events are confined in an upper triangle: with boldface data, if the table is divided by the diagonal into upper and lower parts, only 2% out of the total belongs to the lower triangle which includes only flare classes 3N, 1F, 2F and 3F. This feature of the number distribution of Hα flares implies some essential aspects distinguished from electron events.

Another characteristic feature of proton events may be realized in Table 2. Table 2 shows no such triangle feature. A distinctive character of Table 2 compared with Table 1 is that not all flares which belong to the upper triangle accompany proton events. The fraction in the parenthesis indicates the probability for the Hα flares accompanying proton events. The weaker

the intensity of flare and the smaller its area, the less is the probability of proton events and it is of order 10^{-2} for class SF, whereas it is of order 1 for class 3B and of almost 1 for class 2B.

Table 2 Number Distribution of Total Hα Flares

Hα Flare	S	1	2	3
B	1556 (1/47)	267 (1/3)	62 (1/1.1)	14 (1/1)
N	4032 (1/119)	2912 (1/52)	232 (1/11)	18 (1/9)
F	3559 (1/209)	1211 (1/404)	145 (1/72)	15 (0)

Note: Fraction in parenthesis is the number ratio of proton events accompanying flares to all flares.

As will be elucidated below, the first, peculiar, triangular distribution of proton events seems to be associated with the physics of proton acceleration process, while the second character that emerged from a comparison of Table 1 and Table 2 seems to be ascribable to detection effect. The peculiar proton event distribution shown in Table 1 is a stark fact to be elucidated. Through an interpretation of this characteristic feature we deal with the physics of a possible acceleration mechanism.

3 PROTON ACCELERATION BY DC ELECTRIC FIELD AND FORMATION OF AN ION-ANISOTROPIC DISTRIBUTION

Along with acceleration across magnetic field, acceleration parallel to the magnetic field (by $E_{\parallel}$) must be taken into account. Parallel electric field may be determined by using current helicity deduced from the vector magnetogram of active regions.

According to the general magnetic reconnection theory (Schindler et al. 1988), only in resistive diffusion region of magnetized plasma can the parallel electric field exist. The parallel electric field may be estimated by the following approximate formula (see Appendix):

$$E_{\parallel} \simeq \frac{h_{\rm c}}{\mu_0 B_0 \sigma}\,, \tag{1}$$

where $h_{\rm c}$ is the density of electric current helicity , σ, the conductivity, B_0, the magnetic field, and μ_0, the permeability of free space. Observations of vector magnetic field make it possible to determine the current helicity at the photosphere level (Bao et al. 1999). Let us choose a representative value of the current helicity $h_{\rm c} \simeq 5 \times 10^{-3}\,{\rm G}^2\ {\rm m}^{-1}$ and Spitzer conductivity $\sigma = 10^{-3} T^{1.5}$ (Siemens $\rm m^{-1}$). For the representative values above the photosphere, $T \simeq 10^4\,{\rm K}$ and $B_0 \simeq 100\,{\rm G}$, we obtain $E_{\parallel} \simeq 4 \times 10^{-2}\ {\rm V\,m^{-1}}$. On the other hand, a representative perpendicular electric field $E_{\perp} \simeq 10^3\ {\rm V\,m^{-1}}$ (Martens 1988). The parallel electric field $E_{\parallel}$ is weaker by five orders of magnitude than the perpendicular field $E_{\perp}$, so one can neglect the parallel field.

We, accordingly, consider only acceleration across the magnetic field. A most suitable scenario for prolonged acceleration of particles seems to be the following (Martens 1988; Benz 1994; Akimov et al. 1994; Litvinenko & Somov 1995; Litvinenko 1996):

During the post-impulsive phase the magnetic field above the active region, strongly disturbed by a CME, relaxes to its initial state through magnetic reconnection. Then, a current sheet can be formed behind the rising CME. This current sheet would become the seat of particle acceleration by a pertinent mechanism.

One of the feasible mechanisms is acceleration by DC electric field.

Another scenario of particle acceleration by DC electric field is acceleration in flare seat by an explosive coalescence of two approaching loop systems (de Jager & Sakai 1991; Sakai & de Jager 1991; Sakai 1992). Through a numerical simulation Sakai (1992) showed the high effectiveness of particle acceleration by DC electric field in a coalescence of two loop systems. According to the simulation, on explosive coalescence the electric field abruptly increases by as much as 10^4 times during a few seconds, and this leads to the acceleration of protons up to 10 GeV for a millisecond.

Their approach, however, is one of MHD, so they could not reveal the kinetic effects in the reconnecting current sheet. Flare initiation and development cannot be understood without taking into account kinetic and microturbulent phenomena in current sheet (Priest & Forbes 2000). After triggering, flares are thought to develop various kinds of cascading MHD turbulence (LaRosa & Moore 1993; LaRosa et al. 1994; Miller et al. 1997). Thus the reconnecting current sheet would become a seat of competition between micro- and macroturbulence and DC electric field. In order to check the effectiveness of two acceleration mechanisms, one can compare their respective acceleration characteristic time (ACT) for each particle species. The comparison shows that the ACTs for electrons are of the same order of magnitude for both mechanisms while the ACTs for protons differ as much as $10^4 - 10^5$ times, with the ACT by DC field being the shorter. This means that protons near the reconnecting current sheet (RCS) are preferentially accelerated by DC electric field alone.

Consequently, we accept the concept that protons are accelerated by DC electric field in the impulsive and prolonged post-impulsive phase, and only strong flares produce additionally accelerated protons in coronal and interplanetary shocks (de Jager 1990; Kahler 1994). Observations clearly showed that flares with a single phase of acceleration as well as with two phases do exist, the former being small flares (Kallenrode & Wibberenz 1991), and yet such small flares can generate accelerated proton beams (see Table 1) which provide the necessary condition for the acceleration (see below).

After a flare is triggered in and near the RCS, the generated DC electric field may be expressed as

$$\boldsymbol{E} = \boldsymbol{j}/\sigma^* - \boldsymbol{V}_\mathrm{d} \times \boldsymbol{B}_0, \tag{2}$$

where $\boldsymbol{V}_\mathrm{d}$ is the drift (inflow) velocity of plasma in magnetic field $\boldsymbol{B}_0$, and σ^* is the anomalous conductivity in the RCS. We adopt the same condition of acceleration as in Martens (1988) and Litvinenko & Somov (1995). The drift velocity V_d ranges from $10^3\,\mathrm{m\ s^{-1}}$ up to $10^7\,\mathrm{m\ s^{-1}}$ (de Jager & Sakai 1991). Hence, $V_\mathrm{d} = 10^3\,\mathrm{m\ s^{-1}}$ gives $E = 10\,\mathrm{Vm^{-1}}$ ($B_0 = 100\,\mathrm{G}$), while $V_\mathrm{d} = 10^7\,\mathrm{m\ s^{-1}}$ gives $E = 10^5\,\mathrm{Vm^{-1}}$. This strength greatly exceeds the Dreicer field in the corona, $E_\mathrm{D} \simeq 10^{-1} - 10^{-5}\,\mathrm{Vm^{-1}}$ (Miroshnichenko 1995; Priest & Forbes 2000), so protons must be accelerated in a runaway regime.

On the other hand, from the same consideration as Martens (1988) one can conclude that proton acceleration in RCS must be in a completely collisionless, runaway regime.

In this regime particles accelerated by field (1) should gain energy only in the plane perpendicular to the magnetic field, and if we can adopt $\varepsilon_\mathrm{k} \simeq \varepsilon_{\mathrm{k}\perp}$, the rate of energy increase of a particle drifting along the DC electric field is given by

$$(\mathrm{d}\varepsilon_\mathrm{k}/\mathrm{d}t)_\mathrm{E} = \chi e E c \sqrt{\varepsilon^2 - m^2c^4}/\varepsilon, \tag{3}$$

where χ is a constant less than 1 and expresses the projection of the particle's path on the direction of the DC field, and ε_k and ε are the kinetic and relativistic energies of the particle.

In the nonrelativistic limit, Eq. (3) may be approximated as

$$(\mathrm{d}\varepsilon_\mathrm{k}/\mathrm{d}t)_\mathrm{E} \;=\; (\sqrt{2}\chi eEc/\sqrt{\varepsilon_0})\sqrt{\epsilon_\mathrm{k}} = \alpha\sqrt{\varepsilon_\mathrm{k}}, \tag{4}$$

$$\alpha \;=\; \sqrt{2}\chi eB_0V_\mathrm{d}/\varepsilon_0\,, \tag{5}$$

where ε_0 is the rest energy of the particle. From Eq. (4) we can deduce the ACT by DC electric field

$$t_\mathrm{E} \;=\; \varepsilon_\mathrm{k}/(\mathrm{d}\varepsilon_\mathrm{k}/\mathrm{d}t)_\mathrm{E} = \varepsilon\varepsilon_\mathrm{k}/(\chi eB_0V_\mathrm{d}\sqrt{\varepsilon^2 - m^2c^4}), \quad \text{(relativistic)} \tag{6}$$

$$t_\mathrm{E} \;=\; \varepsilon_\mathrm{k}/(\mathrm{d}\varepsilon_\mathrm{k}/\mathrm{d}t)_\mathrm{E} = \sqrt{\varepsilon_\mathrm{k}}/\alpha\,. \quad \text{(nonrelativistic)} \tag{7}$$

So far we have implicitly assumed that the RCS where the reconnection occurs is neutral. There is however, no loss of generality because, according to the MHD simulation (Sakai & de Jager 1991; Sakai 1992), in a coalescence of two loops, the initial non-neutral 3D-RCS becomes 1D neutral during the explosive coalescence and particle acceleration is highly effective there.

Next, we should emphasize the necessity of introducing a kinetic effect. The point is that when proton is accelerated in the plane perpendicular to the magnetic field only proton energy in that plane should be increased, so, if we define the relevant temperature $T_\perp$, a temperature anisotropy will be developed in the RCS as long as the interaction of protons with ambient medium may be ignored. The ACT of proton, e.g. by Langmuir turbulence (Melrose 1980) when the energy density of the turbulence in units of the thermal energy density is $w \simeq 0.01\%$, is of the order of 10^{-2} s and 10 s for $\varepsilon_\mathrm{k} = 1\,\mathrm{keV}$ ($T \simeq 10^7\,\mathrm{K}$) and $\varepsilon_k = \varepsilon_0/5 \simeq 200\,\mathrm{MeV}$, respectively.

The maximum staying time of proton in the RCS is of the order of 10^{-3} s and 10^{-1} s for length scales of the RCS 10^6 m and 10^8 m, respectively. A comparison of these magnitudes leads to the conclusion that interaction of the protons with the ambient medium during their stay in the RCS may be ignored.

Consequently, the inequality $\varepsilon_\perp/\varepsilon_\parallel > 1$ or $T_\perp/T_\parallel > 1$ will hold in the proton accelerating RCS. The possibility of an ion-anisotropy forming in the RCS its instability was first discussed by Kim (1993).

4 ION-ANISOTROPY INSTABILITY IN RCS AND A POSSIBLE EXPLANATION OF THE OBSERVED CORRELATION BETWEEN SOLAR PROTON EVENTS AND Hα FLARES

In a fully ionized plasma an anisotropic kinetic distribution of one of the components of the plasma will give rise to a kinetic instability of the plasma. An ion-anisotropy in a plasma with a uniform magnetic field (MF) or without it, produces instabilities of electromagnetic and electrostatic types (Mikhailovsky 1972; Timofeev & Pistunovich 1967). Ion-anisotropic instability in a nonuniform MF as in a RCS seems not to have been studied so far. In Dobrowolny (1968), however, it was shown that the inner region of the RCS may be treated in zero-magnetic field approximation.

Let the gyro-radius of an ion in a uniform MF near the RCS be r_ci and the half-depth of the RCS be h. Then the region where MF may be ignored is given by

$$|x| < \sqrt{r_\mathrm{ci}h}, \tag{8}$$

where x is measured from the neutral surface of the RCS. As is the case in usual RCSs, taking into account $r_{\rm ci} > h$, we have $\sqrt{r_{\rm ci}h} > h$, so one can treat the whole RCS in zero-field approximation, and utilize the result obtained for uniform MF without modification. In an ion-anisotropic plasma where $\varepsilon_\perp > \varepsilon_\parallel$ electromagnetic (nonpotential) disturbances propagating along the MF are unstable. For a disturbance with angular frequency

$$\omega \ll k_\parallel v_{T_{\rm e}}, k_\parallel v_{T_{\rm i}} \tag{9}$$

and characteristic wave number

$$k_\parallel \simeq \omega_{\rm pi}/c, \tag{10}$$

the increment of the instability is given by

$$\gamma = \frac{m_e}{m_{\rm p}} \cdot \frac{v_{T_{\rm e}}}{c} \cdot \omega_{\rm pi}, \tag{11}$$

where $\omega_{\rm pi}$ is the ion plasma frequency. For a number density of ions $n = 10^{16}\,{\rm m}^{-3}$ and temperatures $T_{\rm e} = 10^7\,{\rm K}$, and $10^8\,{\rm K}$ in the RCS, the characteristic times of the instability are

$$\gamma^{-1} = 2.7 \times 10^{-4}{\rm s} \quad (T_{\rm e} = 10^7{\rm K}), \quad 6.8 \times 10^{-5} \quad (T_{\rm e} = 10^8{\rm K})\,. \tag{12}$$

After a flare is triggered, the RCS plasma will suffer from the instability when the ion - anisotropy increases and the following inequality is satisfied

$$\frac{T_\perp}{T_\parallel} \geq 1 + \frac{k_\parallel c^2}{{\omega_{\rm pi}}^2}. \tag{13}$$

Thus, in the RCS two mechanisms would operate: acceleration by DC electric field and ion-anisotropic instability, the former accelerating and the latter annihilating acquired energy. The possibility of the accelerated protons escaping from the RCS, therefore, will depend on the relation between the ACT by DC field and the characteristic time of instability γ^{-1}. Only when the inequality

$$t_{\rm E} < \gamma^{-1} \tag{14}$$

is satisfied can protons be sufficiently accelerated to leave the RCS, and thus to give rise to a proton flare. Otherwise, i.e., when the opposite inequality

$$t_{\rm E} > \gamma^{-1} \tag{15}$$

holds no high-energy proton streams will be observable, and, instead, an electromagnetic plasma turbulence will grow up in the RCS.

The logarithm of ACT (7) (nonrelativistic) is given by

$$\log t_{\rm E} = \log \frac{\sqrt{\varepsilon_0}}{\sqrt{2}\chi e B_0} - \log V_{\rm d} + 0.5 \log \varepsilon_{\rm k}. \tag{16}$$

The dependence of $\log t_{\rm E}$ on $\log \varepsilon_{\rm k}$ is illustrated in Fig. 1.

The ACT-lines for four values of the drift velocity, $V_{\rm d} = 10^3$, 10^4, 10^5 and $10^6\,{\rm m\ s}^{-1}$ and two values of the magnetic field ($B_0 = 100, 500\,{\rm G}$) are drawn. The horizontal lines correspond to the characteristic time of instability γ^{-1} at $T_{\rm e} = 10^7\,{\rm K}$, and $10^8\,{\rm K}$, respectively. The case (14) corresponds to the area beneath the horizontal line γ^{-1}, so only when a state of RCS lies below this line, can the flaring RCS yield a proton flare; otherwise, it cannot. As the figure

shows, the larger the values of B_0 or V_d, the greater possibility of proton flares, because then the ACT-lines shift towards lower part of the diagram.

As seen in formulae (6), (4) and (16), B_0 and V_d exert an identical effect on the ACT; accordingly, we can exchange a value of V_d for a corresponding value of B_0. In Fig. 1 the dashed lines correspond to $B_0 = 500\,\mathrm{G}$.

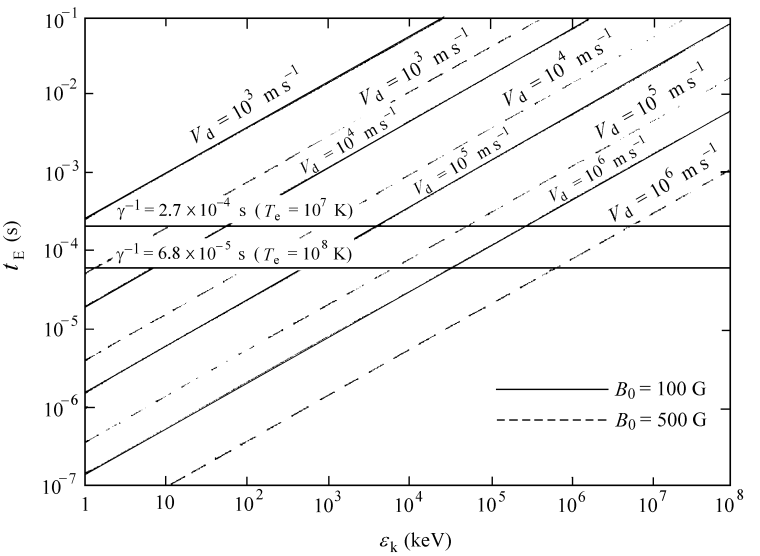

Fig. 1 Acceleration characteristic time by DC electric field versus kinetic energy of particle. Inclined lines correspond to different inflow velocities of magnetic field for two cases, 100 G (solid line) and 500 G (dashed line). The characteristic times of ion-anisotropic instability for $T_\mathrm{e} = 10^7$ K and 10^8 K in the reconnecting current sheet are marked by the two lines parallel to the abscissa.

Now, it must be shown how Fig. 1 makes it possible to interpret the distinct "triangle" feature of Table 1.

First of all, one has to determine which factors determining the ACT by DC electric field are associated with the area (S, 1, 2, 3) and the intensity (B, N, F) of the Hα flare. The intensity of the Hα flare should depend on the power of the reconnection which, in turn, depends directly on the B_0 and V_d.

Assume tentatively a correspondence between the Hα flare intensity and the inflow velocity V_d, as given in Table 3 for $B_0 = 100\,\mathrm{G}$.

Table 3 Correspondence between Hα-intensity and Inflow Velocity V_d

Hα Flare	V_d (m s^{-1}) ($B_0 = 100\,\mathrm{G}$)
B	$10^5 \sim 5.0 \times 10^5$
N	$2.0 \times 10^4 \sim 10^5$
F	$5.0 \times 10^3 \sim 2.0 \times 10^4$

Strictly speaking, the relation between B_0 and V_d must be determined by the dynamics of RCS in a reconnecting circumstance (Schindler et al. 1988), but the identical role of the B_0 and V_d in the ACT (16) makes above the correspondence allowable.

Further, taking into account that an Hα flare site is connected with the original flare site in the lower corona by MF lines, the area signature S, 1, 2 and 3 of Hα flares observed in the lower chromosphere will be correlated with the length of the RCS situated in the coronal flare site, so we can assume that the area of the Hα flare site is roughly proportional to the length of the RCS.

Under constant B_0 and V_d the kinetic energy of a particle will increase with the distance traveled, and the average kinetic energy of a particle when it escapes from the RCS will be proportional to the length of the RCS. If we assume that the abscissa $\log \varepsilon_\mathrm{k}$ in Fig. 1 is logarithm of average kinetic energy of particle escaping from the RCS, then we can tie uniquely the abscissa to the length of the RCS, provided B_0 and V_d are constant. The acquired kinetic energy of a particle ε_k relates to the acceleration length of the particle L in the RCS by the equation:

$$L = \varepsilon_\mathrm{k}\left(\frac{c}{eV_\mathrm{d}B_0}\right). \tag{17}$$

Now, draw under the diagram of Fig. 1 (see Fig. 2) three equally spaced straight lines parallel to the abscissa representing the acceleration length of the particles in the RCS corresponding to the Hα flare intensity F, N and B, respectively. Mark on them the length of RCS calculated by (17) for each line. As the first of three lines corresponds to F, the second to N and the third to B, the points a, b and c on the L-lines should correspond to A, B and C on the ACT-lines, respectively, and the points a′, b′ and c′ on the L-lines, to A′, B′ and C′ on the ACT-lines, etc. Having connected the points A, B, C and A′, B′, C′ etc. respectively, these lines correspond to events where the acceleration length are identical. The lines ABC, A′B′C′, A″B″C″ $\cdots$, therefore, may be considered to correspond to events where the area of the Hα flare have definite, increasing values, e.g., S, 1, 2, $\cdots$.

Thus in the diagram $(\lg \varepsilon_\mathrm{k} - \lg t_\mathrm{E})$ the inclined columns ABC, A′B′C′, A″B″C″ $\cdots$ are expected to correspond to the columns in Table 1. In Fig. 2 the columns ABC, A′B′C′, A″B″C″ $\cdots$ corresponding to S, 1, 2 and 3 of Hα flare are assumed to have the length of the RCS approximately $2.5 \times 10^2 \sim 10^3$, $10^3 \sim 2.5 \times 10^3$, $2.5 \times 10^3 \sim 10^4$, $10^4 \sim 2.5 \times 10^4$ m, respectively.

It should be pointed out here that the three lines under the ($\lg \varepsilon_\mathrm{k}$-$\lg t_\mathrm{E}$) diagram in Fig. 2 do not represent the actual length of the RCS, rather, they represent the average length over which particles are to be accelerated; and the numerical values on the three L-lines must be less than the actual lengths of the RCS.

In fact, a RCS region has its own length L, height (width) H and thickness for a flare. The length L corresponds to the area of H_α flare, as seen above, while the height H might, to some extent, correspond to the intensity of H_α flare, because the rate of inflow of electromagnetic energy into RCS per unit length is the Poynting flux $V_\mathrm{d}B_0^2H/\mu_0$ (Priest & Forbes 2000). However, our formalism does not include the length H; instead, we have only V_d and B_0 in formula (16). In the Poynting flux above, the inflow velocity V_d and height H enter with the same status. We may replace, therefore, a change of the height by a change of the inflow velocity.

In consequence, the characteristic feature of the number distribution in Table 1 seems to be correctly reproduced by the triangle under the γ^{-1}-line in Fig. 2.

Consider now the second aspect of proton events mentioned in Sect. 2. The lower energy limit of detecting protons is 10 MeV. The energy 10 MeV in Fig. 2 corresponds to 2B box. The probability of 2B in Table 2 is almost 1. In the upper triangle where proton events are possible,

the boxes further away from 2B have less probabilities of proton events occurring, because those boxes are further from the lowest energy limit capable of detecting proton events.

The reason that proton events in those boxes have been detected with less probabilities, though, is that sometimes a large flare which has a sufficiently long acceleration length in the coronal flaring site is connected with an Hα flare of shorter length in the chromosphere through MF lines.

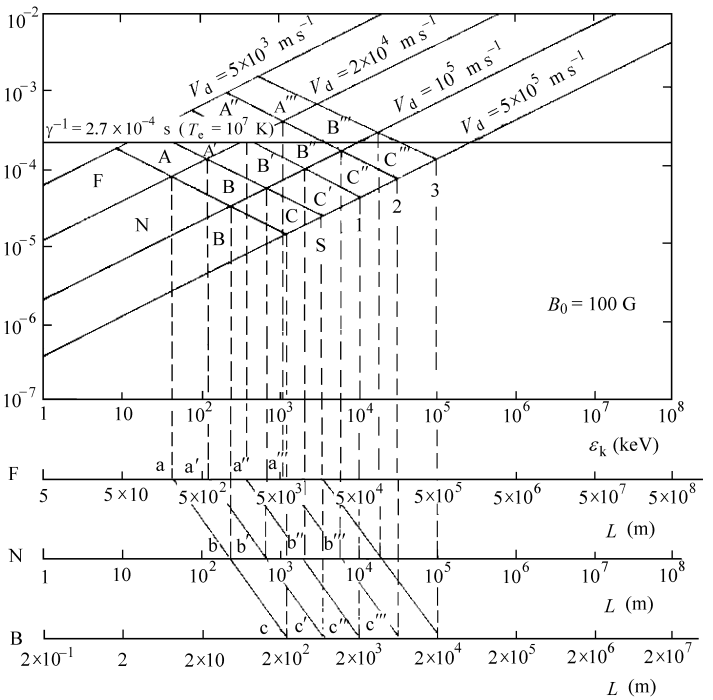

Fig. 2 Same diagram as Fig. 1. Under the diagram, three equally spaced lines represent the acceleration length of a particle in the reconnection current sheet for the three Hα flare intensities, F, N and B.

Further extending the energy range of detector downwards is expected to increase the probability of detection of proton events even in classes 1B, 1N, SB, SN and SF, whereas no such increase is expected in classes 1F, 2F, 3N and 3F.

5 CONCLUSIONS

A comparison of space proton events with related Hα flares has led to the following conclusions:

(1) The number distribution of proton events-related Hα flares in the Hα area versus intensity diagram shows that proton flares are possible only in the upper triangle above the diagonal spanning 3B and SF; (2) the farther Hα box from the lowest energy limit of detector(2B), the less the probability detection of proton events; (3) in RCS where protons are accelerated, ion-anisotropy is built up; (4) in RCS where protons are accelerated, both DC electric field

acceleration and ion-anisotropic instability operate, and only when the ACT by DC electric field is less than the characteristic time for ion anisotropic instability, can proton flare occur; (5) using the electric current helicity deduced from vector magnetograms of active regions, the parallel electric field $E_\parallel$ in the region can be estimated, and it is negligible compared with $E_\perp$; (6) the possibility of protons being accelerated in coronal and interplanetary shocks is not excluded: such shocks can be produced in strong flares, such as 3B, 2B accompanying CME, so such events do not affect our diagram of Table 1.

Acknowledgements This work was carried out during visit of K. J. Su, K. K. Sok and K. J. Song at Huairou Solar Observing Station and could be completed only thanks to the current helicity data of the Station. K. J. Su, K. K. Sok and K. J. Song are thankful to the staff of the Station for providing the current helicity data and for helpful discussion. We are very grateful to an anonymous referee for helpful comments and suggestions. This work was supported by Chinese Academy of Sciences and the Third World Academy of Sciences (TWAS), and partly supported by the National Natural Science Foundation of China.

APPENDIX: Derivation of Parallel Electric Field from Electric Current Helicity

Schindler et al. (1988) have shown in their general magnetic reconnection theory that the component ($E_\parallel$) of electric field along a particular magnetic field line is associated with nonidealness of plasma. On the other hand, the nonidealness promotes a change of magnetic helicity of the magnetized plasma (Priest & Forbes 2000). In a gauge such that $\nabla \cdot \boldsymbol{A}_\mathrm{p} = 0$ and $\boldsymbol{A}_\mathrm{p} \cdot \hat{\boldsymbol{n}} = 0$ on the surface of the system, the time variation of the magnetic helicity is given by

$$\frac{\mathrm{d}H_\mathrm{m}}{\mathrm{d}t} = -2\int_v \frac{\boldsymbol{j}\cdot\boldsymbol{B}}{\sigma}\mathrm{d}V + 2\int_s [(\boldsymbol{B}\cdot\boldsymbol{A}_\mathrm{p})(\boldsymbol{V}\cdot\hat{\boldsymbol{n}}) - (\boldsymbol{V}\cdot\boldsymbol{A}_\mathrm{p})(\boldsymbol{B}\cdot\hat{\boldsymbol{n}})]\mathrm{d}S. \tag{A1}$$

If we could ignore a variation of the magnetic helicity due to the surface term in (A1), the change of the helicity would be expressed by the first term of right side alone.

If we choose some reference time and its corresponding field, and assume that the field does not change on the surface, we find following equation on the magnetic helicity change:

$$\frac{\mathrm{d}H_\mathrm{m}}{\mathrm{d}t} = -2\int_{D_\mathrm{R}} \boldsymbol{E}\cdot\boldsymbol{B}\mathrm{d}V, \tag{A2}$$

where D_R denotes the nonideal region.

Assuming that the nonidealness is uniform in the region, we find a simple relation between the magnetic helicity variation and current helicity

$$\frac{\mathrm{d}H_\mathrm{m}}{\mathrm{d}t} = -\frac{2H_\mathrm{c}}{\mu_0\sigma}. \tag{A3}$$

From (A2) and (A3), we get

$$H_\mathrm{c} = \mu_0\sigma\int_{D_\mathrm{R}} \boldsymbol{E}\cdot\boldsymbol{B}\mathrm{d}V. \tag{A4}$$

This equation shows a relation between $E_\parallel$ and H_c, provided the above conditions hold.

References

Akimov V. V., et al., 1991, 22nd Int. Cosmic Ray Conf. 2, 483
Akimov V. V., Leikov N. G., Belov A. V. et al., 1994, In: J. M. Ryan, W. T. Vestrnd, eds., AIP Conf. Proc. No. 294, High Energy Solar Phenomena, New York: AIP, 106
Alfven H., 1981, Cosmic Plasma, Dordrecht: Reidel
Bao S., Zhang H., Ai G. et al., 1999, A&AS, 139, 311
Barbosa D. D., 1979, ApJ, 233, 383
Benz A. O. et al., 1994, Solar Phys., 153, 33
de Jager C., 1990, Adv. Space Res., 10, 101
de Jager C., Sakai J., 1991, Solar Phys., 133, 395
Dobrovolnyi M., 1968, Neovo Cimento, 55B, 427
Ellison M. A., McKenna S. M. P., Reid J. H., 1961, Dunsink Obs. Publ., 1, 53
Forrest G. J., Chupp E. L., 1983, Nature, 305, 291
Goldman M. V., Smith D. F., 1986, In: P. A. Sturrock, ed., Physics of the Sun, 2, Dordrecht: Reidel, 325
Kahler S., 1994, ApJ, 428, 837
Kallenrode M. B., Wibberenz G., 1991, ApJ, 376, 787
Kim J. S., 1993, Science Bull. of D. P. R. Korea, 4, 31
Kocharov L., Torsti J., Laitinen T., Teittinen N., 1999, Solar Phys., 190, 295
LaRosa T. N., Moor R. L., 1993, ApJ, 418, 912
LaRosa T. N., Moor R. L., Shore S. N., 1994, ApJ, 425, 856
Li W. B., Wang J. X., 1994, Chinese J. Space Sci., 13, 1
Litvinenko Y. E., 1996, ApJ, 462, 996
Litvinenko Y. E., Somov B. V., 1995, Solar Phys., 158, 317
Liu S. P., Li W., 1990, Publ. Yunnan Obser., 4, 75
Martens P. C. H., 1988, ApJ, 330, L131
McGuire R. E., Von Rosenbinge T. T., McDonald F. B., 1981, In: Proc. 17th Int. Cosmic Ray Conf. 3, Paris, 65
Melrose D. B., 1980, Plasma Astrophysics, 2, New York: Gorden & Breach
Mikhailovsky A. B., 1972, In: M. A. Leontovich, ed., Voprosy teorii plazmy, 6, Mockva: Nauka, 70
Miller J. A., et al., 1997, J. Geophys. Res., 102, 14631
Miroshnichenko L. J., 1995, Solar Phys., 156 , 119
Molchanov A. P., ed., 1984, In: Prognozirovanie Solnechnykh Vspyshek iikh Posledstvii, 5, Leningrad: LGU, 108
Pacini F., 1975, In: J. L. Osborne, A. W. Wolfendde, eds., Origin of Cosmic Ray, Dordrecht: Reidel, 371
Priest E., Forbes T., 2000, Magnetic Reconnection, Cambridge: Cambridge Univ. Press
Ramaty R., 1979, In: J. Arons, C. McKee and C. Max, eds., Particle Acceleration Mechanism in Astrophysics, New York: Amer. Inst. of Physics, 135
Sakai J., 1992, Solar Phys., 140, 99
Sakai J., de Jager C., 1991, Solar Phys., 133, 395
Schindler K., Hesse M., Birn J., 1988, J. Geophys. Res., 93, 5547
Schindler K., Hesse M., Birn J., 1991, ApJ, 380, 293
Švestka Z., 1981, In: E. Priest, ed., Solar Flare Magnetohydrodynamics, 1, Dordrecht: Reidel, 47
Švestka Z., Fritzova-Švestkova L., Solar Phys., 36, 417
Švestka Z., Simon P., eds., 1976, Catalog of Solar Particle Events, 1956–1969, Dordrecht: Ridel
Timofeev A. V., Pistunovich V. J., 1967, In: M. A. Leontovich, ed., Voprosy Teorii Plazmy, 5, Mockva: Nauka, 351
Vitinsky Yu. I., ed., 1970-1981, Solnechnye Dannye, 1970-1980, Leningrad: Nauka
Zhang H., Ai G., Li J. et al., 1990, Publ. Yunnan Obs., 4, 64
Zhou S., Zheng X., 1998, Solar Phys., 181, 327